

Study of Orthoexciton-to-Paraexciton Conversion in Cu_2O by Excitonic Lyman Spectroscopy

M. Kubouchi,¹ K. Yoshioka,¹ R. Shimano,^{1,*} A. Mysyrowicz,² and M. Kuwata-Gonokami^{1,†}

¹*Department of Applied Physics, The University of Tokyo, and Solution Oriented Research for Science and Technology (SORST), JST, 7-3-1 Hongo, Bunkyo-ku, Tokyo 113-8656, Japan*

²*Laboratoire d'Optique Appliquée, ENSTA, Ecole Polytechnique, Palaiseau, France*

(Received 23 July 2004; published 6 January 2005)

Using time-resolved $1s$ - $2p$ excitonic Lyman spectroscopy, we study the orthoexciton-to-paraexciton transfer, following the creation of a high density population of ultracold $1s$ orthoexcitons by resonant two-photon excitation with femtosecond pulses. An observed fast exciton-density dependent conversion rate is attributed to spin exchange between pairs of orthoexcitons. Implication of these results on the feasibility of Bose-Einstein condensation of paraexcitons in Cu_2O is discussed.

DOI: 10.1103/PhysRevLett.94.016403

PACS numbers: 71.35.Lk, 71.35.Cc, 78.47.+p

The observation of Bose-Einstein condensation (BEC) of neutral atoms, more than 70 years after its prediction, constitutes a major advance in physics of the last decade [1,2]. Ensembles of ultracold atoms with high controllability of density, temperature, and interaction strength reveals new aspects of many body quantum phenomena. In particular, by applying a magnetic field one can control the sign and magnitude of the scattering length between atoms. This allows probing the low temperature transition between collective pairing of fermionic atoms with attractive interaction and BEC of molecularlike bosonic entities [3]. Excitons, composite particles in semiconductors made of fermions, may provide another system particularly well suited for the study of this transition in a slightly different context. With increasing densities, the fluid should evolve continuously from a dilute Bose-Einstein condensate of excitons into a dielectric superfluid consisting of a BCS-like degenerate two-component Fermi system with Coulomb attraction [4,5]. Several recent experimental results have renewed interest in the search of BEC in photo-excited semiconductors [6].

It has long been recognized that Cu_2O provides a material with unique advantages for the observation of BEC of excitons [7]. Because of the positive parity of the valence and conduction band minima at the center of the Brillouin zone, their radiative recombination is forbidden in the dipole approximation, conferring a long radiative lifetime to the $n = 1$ exciton. The $n = 1$ exciton level is split by exchange interaction in a triply degenerate orthoexciton state (symmetry Γ_3^+ ; 2.033 eV at 2 K), and a lower lying singly degenerate paraexciton (Γ_2^+ ; 2.021 eV at 2 K) which is optically inactive to all orders. Several experiments have shown intriguing results in luminescence and transport suggesting the occurrence of a degenerate excitonic quantum fluid at high densities and low temperatures in this material [8,9]. However, a controversy has been raised on the actual density of excitonic particles created by optical pumping. Based on luminescence absolute quantum efficiency measurement, it has been claimed that an Auger effect with a giant cross section destroys excitons when the

density exceeds 10^{15} cm^{-3} , preventing BEC [10]. On the other hand, other authors have shown that another process, orthoexciton-paraexciton conversion by spin exchange, is much more probable at low temperature [11]. Since this last effect does not destroy excitons, but merely increases the orthoexciton-paraexciton conversion rate, it does not prevent BEC. To resolve this controversy, it is of prime importance therefore to explore the ortho-para conversion rate as a function of density. More generally, it is important to study the dynamics of paraexcitons in order to optimize the pumping conditions to achieve BEC. One of the major difficulties in this respect was the lack up to now of a sensitive spectroscopic method to probe optically inactive paraexcitons.

In this Letter, we use a new spectroscopic approach to study the dynamics of orthoexciton-paraexciton conversion in Cu_2O . The technique consists of probing the transition from the populated $1s$ to the $2p$ state, with a midinfrared (MIR) light beam. MIR excitonic spectroscopy is the counterpart of Lyman spectroscopy in atomic hydrogen [12–14]. It is especially well suited for the study of paraexcitons in Cu_2O because the $1s$ - $2p$ transition is allowed even if the $1s$ paraexciton is optically inactive. With the use of a short pump pulse to excite orthoexciton and a weak MIR short probe light pulse, one can follow the gradual buildup of the paraexciton population from the ortho-para conversion and its subsequent decay. Since the dipole matrix element for the $1s$ - $2p$ transition is known, one can extract the density of paraexcitons from the strength of the Lyman absorption. This has to be contrasted with luminescence data, where exciton-density estimates rely on measurements of absolute radiative quantum efficiency, a notoriously difficult task. In addition, the line shape of Lyman absorption yields precise information on the energy distribution of $1s$ excitons. In particular, Johnsen and Kavoulakis pointed out that it should show a characteristic abrupt change when excitonic BEC occurs [14].

To follow the density and temperature evolution of the orthoexcitons and paraexcitons starting with a well con-

trolled situation, we first generate orthoexcitons by resonant two-photon absorption (TPA), using an ultrashort laser pulse. Drawing an analogy with the two-photon excitation of biexcitons in CuCl with ultrashort laser pulses [15], we note that the created orthoexcitons have a very low initial temperature despite the large laser bandwidth, because of the small group velocity dispersion at the TPA laser frequency ($\hbar\omega = 1.0164$ eV). In fact, the initial momentum spread of the generated orthoexcitons is even much smaller than in the case of biexcitons in CuCl. A conservative estimate yields an initial orthoexciton temperature much less than 10^{-3} K.

The experimental setup and a relevant energy diagram are shown in Fig. 1. A 150 fs laser pulse tunable around 1220 nm provides the pump source. A tunable light pulse in the MIR around $10\ \mu\text{m}$ provides the weak probe source. The $170\ \mu\text{m}$ thick single crystal platelets were cooled by contact with a liquid helium bath. Unless otherwise specified, the pump laser was propagating along a [100] crystal axis.

Representative Lyman absorption spectra are shown in Fig. 2 at various pump-probe delays ranging between -10 and 800 ps. Figure 2(a) is obtained with two-photon resonant excitation using a pump pulse energy of $1.0\ \mu\text{J}$ focused on a spot diameter of $400\ \mu\text{m}$ ($0.81\ \text{mJ}/\text{cm}^2$), corresponding to an intensity of $5.4\ \text{GW}/\text{cm}^2$ and an estimated initial orthoexciton density of about $10^{16}\ \text{cm}^{-3}$ assuming a two-photon absorption coefficient of $\beta = 0.001\ \text{cm}/\text{MW}$ [16]. Figure 2(b) is obtained by tuning the pump pulse to $600\ \text{nm}$, inside the phonon-assisted absorption edge of the $n = 1$ orthoexciton. Because the exciton hyperfine splitting is large ($12\ \text{meV}$) for the $n = 1$ level and negligibly small (much smaller than the experimental limit of the spectral resolution $0.3\ \text{meV}$) for the $n = 2$ level, one can record simultaneously the Lyman transition for orthoexcitons and paraexcitons. Under both pumping conditions, two lines appear around 116 and $129\ \text{meV}$,

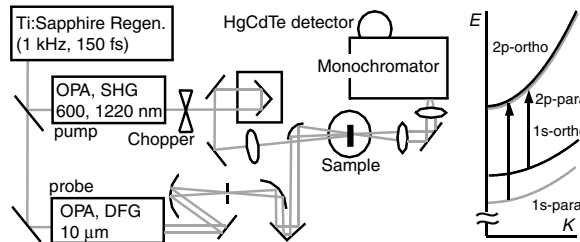


FIG. 1. Experimental setup for time-resolved pump-probe spectroscopy of excitonic Lyman transitions. The 150 fs duration pump pulse is obtained from a Ti:sapphire laser and optical parametric amplifier. The pump pulse wavelength can be tuned around 1220 or 600 nm. The midinfrared probe pulse, of the same duration, is obtained by parametric down-conversion. It is tunable around $10\ \mu\text{m}$. On the right hand side, the energy diagram of the relevant levels is shown.

exactly where the $1s$ - $2p$ Lyman transitions of the orthoexcitons and paraexcitons are expected [17].

We have carefully verified that the appearance of a signal at the position of the paraexciton line at $129\ \text{meV}$ in Fig. 2(a) is not simply due to the direct creation of paraexcitons by the pump pulse, using the following measurements. First, it was verified that both lines at 116 and $129\ \text{meV}$ disappear if the pump frequency is tuned off orthoexciton resonance. Second, we have measured their polarization dependence as a function of the pump polarization vector, for two different directions of propagation with respect to the crystal axes (see Fig. 3). As mentioned before, the two-photon absorption to the paraexciton is forbidden so that no polarization dependence can be assigned to such a transition. One expects, for the orthoexciton state Γ_5^+ , a dependence of the two-photon absorption with the polarization angle of the form [18,19]

$$\Delta\alpha \propto \sin^2 2\theta, \quad (1)$$

if $k \parallel [100]$, and

$$\Delta\alpha \propto \sin^2 2\theta + \sin^4 \theta, \quad (2)$$

for $k \parallel [110]$. Where $\Delta\alpha$ is the induced absorption, θ is the angle between the polarization vector and the crystal axis [001] and the k vector points along the laser beam direction. The observed behavior for both lines at 116 and $129\ \text{meV}$ are the same, as shown in Fig. 3, and it exhibits the polarization dependence expected for a two-photon

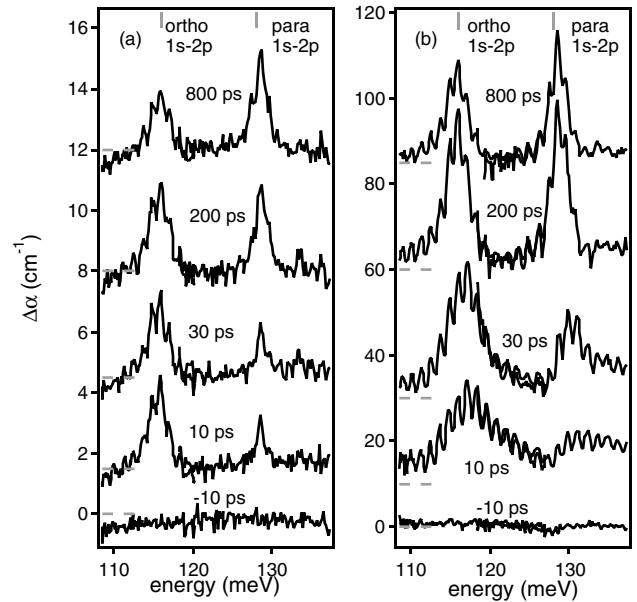


FIG. 2. (a) Lyman absorption recorded in a $170\ \mu\text{m}$ thick single crystal of Cu_2O held at $4.2\ \text{K}$ at different delays from the pump beam. The pump beam tuned at $1220\ \text{nm}$ (two-photon resonant excitation of the orthoexciton) is incident along a [100] crystal axis. (b) Same as in (a), except for the pump wavelength, now tuned at $600\ \text{nm}$ (nonresonant one-photon excitation of orthoexcitons).

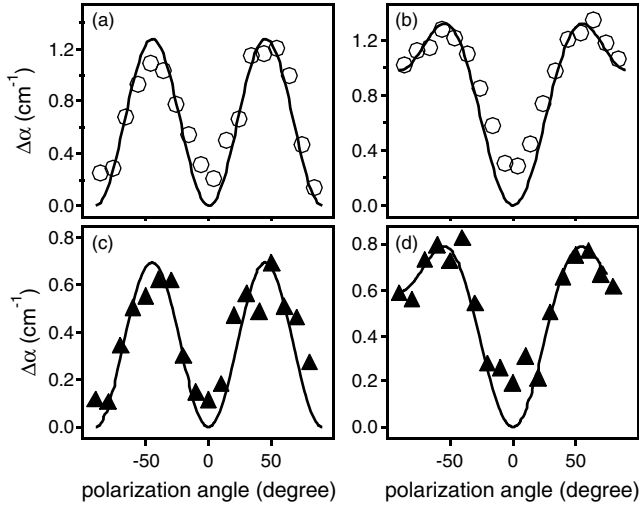


FIG. 3. Lyman absorption of orthoexciton (open circles) measured as a function of the angle between the laser polarization and the crystal axis [001], for two crystal orientations: (a) $k \parallel [100]$, and (b) $k \parallel [110]$. The Lyman absorption of paraexciton [closed triangles: (c),(d)] exhibits the same dependence.

transition to the Γ_5^+ orthoexciton state. Both experiments therefore indicate that orthoexcitons are first created by the pump source, and subsequently decay into paraexcitons.

The temporal evolution of the shapes of the two Lyman absorption lines shown in Fig. 2 reflects the dynamics of the distribution functions of orthoexcitons and paraexcitons. At long delay, $\Delta t > 200$ ps, the lines acquire a width corresponding to the lattice temperature both under one-photon and two-photon pumping. At early times, however, there is a significant difference, depending on the type of excitation (one or two photon). In the one-photon excitation, the lines are broader and shifted to higher energies [see Fig. 2(b)]. This signals a higher excitonic effective temperature, due to the excess energy delivered to the exciton gas in the pumping process. With resonant two-photon excitation [see Fig. 2(a)], the phase space compression scheme confers an initial effective temperature to the orthoexciton gas well below that of the lattice, as already mentioned [15].

The time evolution of the orthoexciton and paraexciton densities is shown in more detail within a small [Fig. 4(b)] and a large [Fig. 4(a)] time interval under two-photon resonant excitation of 1s orthoexcitons with a pump pulse energy of 0.81 mJ/cm^2 . One can observe a very fast rise of the line at 129 meV, in less than 1 ps. A different kinetics is observed on a longer time scale. The line population keeps increasing, but at a slower rate while the orthoexciton line at 116 meV decays with a time constant of the order of 1 ns. Figure 5 shows the variation of the paraexciton Lyman absorption at 129 meV on a long time scale at higher pump intensities. Its rise time in the interval 2–100 ps becomes faster when the pump intensity is increased [Fig. 5(a)]. It can be approximately fitted by an

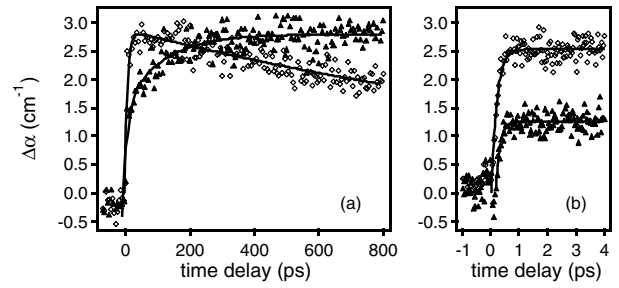


FIG. 4. (a) Kinetics of the Lyman absorption of orthoexcitons (open circles) and paraexcitons (closed triangles) following two-photon resonant excitation of the orthoexciton line. (b) The expanded trace at early time shows the fast rise of the paraexciton population. The crystal temperature is 4.2 K. The excitation density is 0.81 mJ/cm^2 .

exponential, with a laser intensity dependent time constant, as shown in Fig. 5(b).

To discuss the kinetics, we distinguish three characteristic times: picoseconds, 100 ps, and nanoseconds. We start with the slowest process which has recently been discussed comprehensively [20]. From the temperature dependence of the exciton luminescence kinetics, Jang *et al.* have shown that ortho-para conversion occurs via the participation of a transverse acoustic phonon. This mechanism is relatively slow, with a characteristic conversion time of the order of nanoseconds. It is independent of particle density but increases with temperature. The slow decay rate of orthoexcitons with a nanosecond time constant seen in Fig. 4, accompanied by a buildup of paraexcitons at a similar rate, is consistent with this process.

We next consider behavior in the range of 100 ps, where we observe the excitation density dependent increase of the area of the paraexciton Lyman line as shown in Fig. 5. We can exclude the Auger-type process with loss of particles since the areas of orthoexciton and paraexciton signals are almost conserved as we find in Fig. 4. Kavoulakis and Mysyrowicz have proposed a fast orthoexciton-paraexciton conversion effective at high exciton densities and low temperature [11]. It corresponds to an electron spin exchange between two orthoexcitons in a relative singlet spin configuration, resulting in their conversion in two paraexcitons. Such a mechanism scales like

$$\frac{dn_o}{dt} = -Cn_o^2, \quad (3)$$

where n_o is the orthoexciton density and the constant C is evaluated to be of the order of $\sim 5 \times 10^{-16} \text{ cm}^3/\text{ns}$. From the spectral area of its Lyman absorption line, we estimate the orthoexciton density

$$n_o = \frac{\hbar c \sqrt{\epsilon_b}}{4\pi^2 \Delta E_{1s-2p} |\mu_{1s-2p}|^2} \int_0^\infty \Delta \alpha_o(E) dE, \quad (4)$$

where ΔE_{1s-2p} and μ_{1s-2p} are the transition energy and

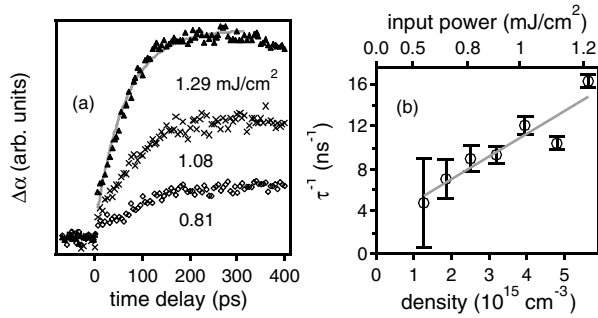


FIG. 5. (a) Variation of the increase of the Lyman absorption of paraexcitons for various pump intensities. The increase of absorption is fitted to an exponential, as shown. (b) The exponential values obtained at different pump laser intensities are shown. The line obeys the relation $\tau^{-1} = a + C_{\text{exp}} n_{\text{ex}}$, with $a = 2.7 \pm 1.4 \text{ ns}^{-1}$ and $C_{\text{exp}} = (2.8 \pm 0.4) \times 10^{-15} \text{ cm}^3/\text{ns}$.

dipole moment of $1s$ - $2p$ transition. The background dielectric function ϵ_b in the frequency of Lyman transition is estimated to be about 7. In our previous paper [17], we took a $1s$ - $2p$ dipole moment of $6.3 e \text{ \AA}$ by direct analogy with the hydrogen atom [21]. For the yellow series of excitons in Cu_2O , we need to take into account the central cell correction effects which reduces the overlap between $1s$ and $2p$ exciton wave functions yielding the revised dipole moment of $1.64 e \text{ \AA}$ [22,23]. The exponential values obtained from the experiment at different pump densities are plotted in Fig. 5(b) as a function of the orthoexciton density estimated from the above formula. From the slope shown in Fig. 5(b), we obtain the constant $C_{\text{exp}} = (2.8 \pm 0.4) \times 10^{-15} \text{ cm}^3/\text{ns}$, a factor of 6 larger than the prediction of Ref. [11]. The spin exchange mechanism therefore provides a convincing scenario to explain the rapid orthoexciton-paraexciton conversion occurring on a 100 ps time scale, when the orthoexciton density exceeds 10^{15} cm^{-3} .

We finally address the initial kinetics, when a narrow line at 129 meV is seen at an orthoexciton density $< 10^{15} \text{ cm}^{-3}$ [Fig. 4(b)]. The spin exchange process is not expected to contribute significantly in such a low density regime. We identify the fast response as being due to the contribution of the $1s$ - $3p$ orthoexciton transition, which accidentally lies close to the $1s$ - $2p$ paraexciton line. In order to confirm this interpretation, experiments should be performed with better spectral resolution at early times, in order to resolve the higher order term $1s$ - $4p$ of the Lyman series.

In conclusion, we have demonstrated a scheme to detect the buildup of paraexcitons following the creation of an ultracold orthoexciton population in Cu_2O . Orthoexciton-paraexciton conversion by spin exchange between pairs of orthoexcitons has been observed. Metastable biexcitons could resonantly enhance the scattering similar to the

Feshbach resonance of cold atoms. The observed enhanced production of spin forbidden paraexcitons from cold orthoexcitons provides a unique opportunity to reach BEC states of excitons.

The authors are grateful to S. Nobuki for experimental support. The authors are also grateful to T. Tayagaki, N. Naka, and Yu. P. Svirko for stimulating discussions. This work is partly supported by the Grant-in-Aid for Scientific Research (S) from Japan Society for the Promotion of Science (JSPS).

*Present address: Department of Physics, The University of Tokyo, Tokyo 113-8656, Japan.

†Electronic address: gonokami@ap.t.u-tokyo.ac.jp

- [1] M. H. Anderson, J. R. Ensher, M. R. Matthews, C. E. Wieman, and E. A. Cornell, *Science* **269**, 198 (1995).
- [2] K. B. Davis, M.-O. Mewes, M. R. Andrews, N. J. van Druten, D. S. Durfee, D. M. Kurn, and W. Ketterle, *Phys. Rev. Lett.* **75**, 3969 (1995).
- [3] C. A. Regal, M. Greiner, and D. S. Jin, *Phys. Rev. Lett.* **92**, 040403 (2004).
- [4] L. V. Keldysh and A. N. Kozlov, *Zh. Eksp. Teor. Fiz.* **54**, 978 (1968) [*Sov. Phys. JETP* **27**, 521 (1968)].
- [5] C. Comte and P. Nozieres, *J. Phys. (Paris)* **43**, 1069 (1982).
- [6] L. V. Butov, A. C. Gossard, and D. S. Chemla, *Nature (London)* **418**, 751 (2002).
- [7] A. Mysyrowicz, *J. Phys. (Paris)* **41**, 281 (1980).
- [8] E. Fortin, S. Fafard, and A. Mysyrowicz, *Phys. Rev. Lett.* **70**, 3951 (1993).
- [9] D. W. Snoke, J. P. Wolfe, and A. Mysyrowicz, *Phys. Rev. B* **41**, 11 171 (1990).
- [10] K. E. O'Hara and J. P. Wolfe, *Phys. Rev. B* **62**, 12909 (2000).
- [11] G. M. Kavoulakis and A. Mysyrowicz, *Phys. Rev. B* **61**, 16619 (2000).
- [12] H. Haken, *Fortschr. Phys.* **38**, 271 (1958).
- [13] S. Nikitine, *J. Phys. Chem. Solids* **45**, 949 (1984).
- [14] K. Johnsen and G. M. Kavoulakis, *Phys. Rev. Lett.* **86**, 858 (2002).
- [15] M. Kuwata-Gonokami, R. Shimano, and A. Mysyrowicz, *J. Phys. Soc. Jpn.* **71**, 1257 (2002).
- [16] A. Jolk, M. Jörger, and C. Klingshirn, *Phys. Rev. B* **65**, 245209 (2002).
- [17] M. Kuwata-Gonokami, M. Kubouchi, R. Shimano, and A. Mysyrowicz, *J. Phys. Soc. Jpn.* **73**, 1065 (2004).
- [18] M. Inoue and Y. Toyozawa, *J. Phys. Soc. Jpn.* **20**, 363 (1965).
- [19] T. R. Bader and A. Gold, *Phys. Rev.* **171**, 997 (1968).
- [20] J. I. Jang, K. E. O'Hara, and J. P. Wolfe, *Phys. Rev. B* **70**, 195205 (2004).
- [21] M. Artoni, G. C. LaRocca, I. Carusotto, and F. Bassani, *Phys. Rev. B* **65**, 235422 (2002).
- [22] G. M. Kavoulakis, Y.-C. Chang, and G. Baym, *Phys. Rev. B* **55**, 7593 (1997).
- [23] M. Jörger, C. T. Fleck, and C. Klingshirn (unpublished).